4. *Ibid.*, 2268 (1955).
5. *Ibid.*, **25**, 624 (1956).
6. Amdur, I., and E. A. Mason, *Phys. Fluids*, **1**, 370 (1958).
7. ———, and J. E. Jordan, *J. Chem. Phys.*, **27**, 527 (1957).
8. Bonilla, C. F., S. J. Wang, and H. Weiner, *Trans. Am. Soc. Mech. Engrs.*, **78**, 1285 (1956).
9. Buckingham, R. A., A. E. Davies, and A. R. Davies, *Proc. Conf. Thermod. Transport Properties Fluids, London*, p. 111 (July, 1957).
10. de Boer, Jan, and R. B. Bird, *Phys. Rev.*, **83**, 1259 (1951).
11. Hartunian, R. A., and P. V. Marrone, *Phys. Fluids*, **4**, 535 (1961).
12. Hirschfelder, J. O., C. F. Curtiss, and R. B. Bird, "Molecular Theory of Gases and Liquids," Wiley, New York (1954).
13. Margenau, H., *Phys. Rev.*, **64**, 131 (1943).
14. *Ibid.*, **66**, 303 (1944).
15. Rossini, F. D., K. S. Pitzer, R. L. Arnett, R. M. Braun, and G. C. Pimental, "Selected Values of Physical and Thermodynamic Properties of Hydrocarbons and Related Compounds," p. 725, Carnegie Press, Pittsburgh, Pa. (1953).
16. Stiel, L. I., and George Thodos, *A.I.Ch.E. Journal*, **7**, 611 (1961).
17. Vanderslice, J. T., Stanley Weissman, E. A. Mason, and R. J. Fallon, *Phys. Fluids*, **5**, 155 (1962).
18. Vasilesco, Virgile, *Ann. Phys.*, **20**, 292 (1945).
19. Yun, Kwang-sik, Stanley Weissman, and E. A. Mason, *Phys. Fluids*, **5**, 672 (1962).

Manuscript received August 10, 1962; revision received March 4, 1963; paper accepted March 8, 1963.

Filtration Behavior of a Mixture of Two Slurries

MOMPEI SHIRATO, MASAO SAMBUICHI, and SAKIO OKAMURA
Nagoya University, Nagoya, Japan

HYDRAULIC PRESSURE AND POROSITY VARIATION

It has long been known that filter cakes are not deposited with uniform porosity. The layers near the medium are compact and dry, and the surface is wet and soupy, indications that the porosity is a minimum at the medium and increases as the cake surface is approached. It has also been known that the hydraulic pressure variation is not linear with distance. In the past ten years attention has been increasingly focused on these effects in relation to various models and theories proposed with respect to the internal nature of filter cakes. Basically, as a fluid flows through a compressible solid, a frictional drag develops which causes nonuniform compaction. The porosity ϵ_x and filtration resistance α_x vary throughout filter cakes, and average values deduced from overall measurements have limited worth. As in the cases of heat exchangers and absorption towers, it is necessary to study local conditions if the fundamental theory is to be elucidated. The Ruth compression-permeability cell (9), combined with apparatus for determining hydraulic pressure distribution described in this paper, affords a basic tool for obtaining data similar to temperature distribution curves in heat transfer apparatus.

When a liquid flows frictionally past the particles in a filter bed, the drag exerted on each particle is communicated to the next particle, and a cumulative effect causes the last layers to be more compact than the first. By means of a force balance (2), the sum of the hydraulic pressure p_x and the solid compressive pressure p_s may be shown to equal the applied filtration pressure in accord with

$$p_x + p_s = p \tag{1}$$

One of the most important postulates of filtration states that the porosity and filtration resistances, determined under a given mechanical loading p_s in a compression-permeability cell, are the same as the porosity and resistance at a point where the cake compressive pressure equals the mechanical loading in the cell.

Whereas p_s is measured directly in the compression-permeability cell, it can be calculated only indirectly in the filter cake by means of Equation (1) with the directly measurable quantities p and p_x. The compression permeability cell essentially consists of a cake contained between two rigid porous plates. After application of any desired cake pressure p_s to the movable upper plate, the solid is allowed to reach an equilibrium porosity; liquid is then permitted to flow through the bed under a low head so that the permeability or filtration resistance can be determined. At some point in the solid, the liquid pressure has dropped from the applied pressure p to a local value of p_x.

In accordance with the force-balance equation, the cake pressure p_s may be calculated by means of $p_s = p - p_x$. At this point α_x and ϵ_x are assumed to be the same in the filter cake and compression-permeability cell. When porosity is measured in a cell, a definite period of time ranging from a few minutes to several hours (5 to 20 min. being common) is required to reach equilibrium. If the filtration is performed under the conditions of rapid cake buildup, sudden change of pressure or rate, or oscillation

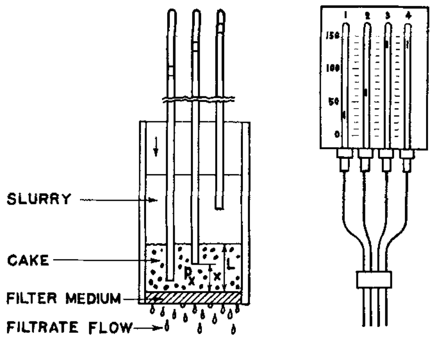

Fig. 1. Schematic view of air-sealed manometers.

of applied pressure (as may occur when using a positive displacement pump), the basic equivalence of equilibrium conditions in the cell and filter cake will not be realized.

MEASUREMENT OF HYDRAULIC PRESSURE VARIATION

The direct determination of porosities at different positions in a cake would be time consuming, tedious, and probably inaccurate. An indirect method, consequently, was employed in which the liquid pressure drop was determined as a function of the distance through the solid. With the hydraulic pressure p_x known, the cake compressive pressure p_s can be calculated by using equation $p_s = p - p_x$. Knowing p_s, one can estimate the porosity distribution from compression-cell measurements.

In Figure 1 the experimental apparatus for determining the liquid pressure distribution is pictured. On the left is the arrangement of probes as they are placed in the cake. Placing them parallel rather than perpendicular to the flow results in minimum disturbance of the filter bed. In actual operation, it was essential to avoid completely vibration of the probes submerged in slurry to prevent channels from developing along the probes with resulting erratic pressure readings. The upper parts of the probes formed a part of the air-sealed manometers shown on the right in Figure 1. These manometers consisted of seven glass capillaries, 0.35 mm. I.D., 3.0 mm. O.D., and approximately 150 mm. long. One end of each capillary was sealed after a column of mercury, approximately 10 mm. in length, had been introduced in the other end. Each capillary was connected to one end of a brass tube 2.5 mm. I.D., by means of a special fitting consisting of four parts, namely the body of the fitting, a rubber gasket, a gland to retain the gasket, and a cap nut to retain the gland. The other ends of these brass tubes were affixed so as to form a cluster, each tube being approximately 2 to 3 mm. consecutively shorter than the longest tube. Thus fairly accurate measurements of the hydraulic pressures at different positions within the filter cake were ensured. The inside diameter of capillaries was limited and controlled by the behavior of the mercury within the tube and was the smallest diameter that would permit the mercury to move uniformly. With a very long hypodermic needle and syringe, the brass tubes were completely filled with water to reduce to a minimum the amount of slurry that could enter the tubes when the filtration pressure was applied. The air in the sealed manometers of Figure 1 was compressed as the mercury moved upward, the position of the mercury column being calibrated against known pressures. The tubes had to be cleaned frequently, and calibrations were repeated each time the manometers were changed.

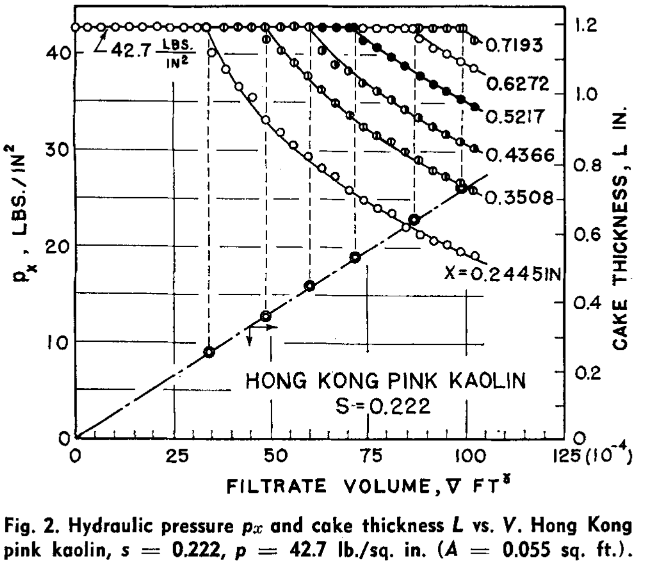

Fig. 2. Hydraulic pressure p_x and cake thickness L vs. V. Hong Kong pink kaolin, $s = 0.222$, $p = 42.7$ lb./sq. in. ($A = 0.055$ sq. ft.).

Results obtained with the setup shown in Figure 1 are presented in Figure 2, where pressure and cake thickness are plotted against filtrate volume at different probe heights for Hong Kong pink kaolin filtered at a constant pressure of 42.7 lb./sq. in. As long as the probe was in the slurry, the pressure remained constant at 42.7 lb./sq. in. However, as soon as cake formed around the probe, the pressure began to fall as shown. In addition to obtaining a set of pressure distribution curves, it was possible to obtain the cake thickness as a function of time. When the cake thickness and filtrate volume are known, the average porosity can be calculated.

THEORIES FOR PREDICTING HYDRAULIC PRESSURE DISTRIBUTION

On the basis of data obtained in runs similar to the one illustrated in Figure 2, p_x and ϵ_x curves of a cement material cake filtered at a constant pressure of 7.11 lb./sq. in. were plotted in Figure 3. The values of porosity were derived indirectly from ϵ vs. p_s data obtained in compression experiments. For a given pressure, the porosity plots were approximately a unique function of x/L, as shown in Figure 3. It has been known (*3*, *10*) that p_x can be related to x/L by the expression

$$\frac{x}{L} = \frac{\displaystyle\int_{p_1}^{p_x} \frac{dp_x}{\alpha_x(1-\epsilon_x)}}{\displaystyle\int_{p_1}^{p} \frac{dp_x}{\alpha_x(1-\epsilon_x)}} \qquad (2)$$

The normalized distance x/L is a function of p_x, and $p_1 = \mu R_m q_1/g_c$ according to Equation (2). Derivation of Equation (2) depends upon the assumption of constant flow rate q throughout the cake, and consequently Equation (2) is limited to filtrations in which the q variation is limited. Normally the flow rate does not vary greatly if the slurry concentration is not high. When p_1 is small enough to be neglected, p_x is a unique function of x/L according to Equation (2).

Calculations involving Equation (2) require a knowledge of local values of both α_x and ϵ_x. Equation (2) may be reduced to an expression in which only porosity data are needed (*11*) if it is assumed that α_x can be expressed as a function of ϵ_x:

$$\alpha_x = \frac{kS_0^2}{p_s}\cdot\frac{1-\epsilon_x}{\epsilon_x^3} \qquad (3)$$

Assuming kS_0^2 to be constant and substituting Equation (3) in Equation (2) yield

$$\left(\frac{x}{L}\right)' = \frac{\displaystyle\int_{0}^{p_x} \frac{\epsilon_x^3}{(1-\epsilon_x)^2}\,dp_x}{\displaystyle\int_{0}^{p} \frac{\epsilon_x^3}{(1-\epsilon_x)^2}\,dp_x} \qquad (4)$$

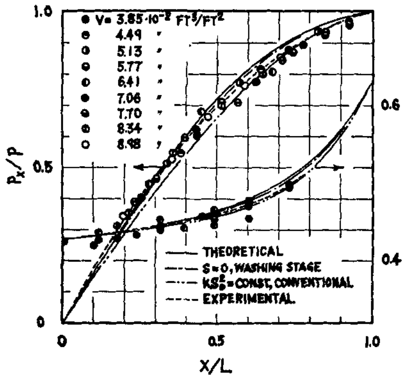

Fig. 3. Hydraulic pressure and porosity distribution in *A* cake. Cement material, $s = 0.384$, $p = 7.11$ lb./sq. in.

when it is assumed that $p_1 = 0$. Equation (4) is interesting in that there is no necessity to make permeability tests in order to calculate the p_x and ϵ_x distributions. Tiller and Cooper (*14*) presented approximate analytical expressions for the relation of p_x to x/L based on the validity of power function relationship of α_x to ϵ_x.

Tiller and Cooper (*13*) pointed out the variation of internal flow rate q_x throughout the cake and derived a relationship between rates of porosity change and internal flow rate in accord with the equation

$$\frac{\partial q_x}{\partial x} = \frac{\partial \epsilon_x}{\partial \theta} \tag{5}$$

Equation (5) forms the basis for modern filtration theory. Starting from Equation (5) and assuming that ϵ_x is solely a function of x/L, Tiller and Shirato (*15*) recently derived a relationship for calculating q_x vs. x/L:

$$\frac{q_x}{q_1} = 1 - \frac{(\epsilon_x - \epsilon_{\text{avg}\,x})(m-1)\,s}{\epsilon_{\text{avg}}(1-ms)} \cdot \frac{x}{L} \tag{6}$$

When $x/L = 1$, $q_x = q_i$, the flow rate in an infinitesimal surface layer, Equation (6) becomes

$$\frac{q_i}{q_1} = 1 - \frac{(\epsilon_i - \epsilon_{\text{avg}})(m-1)\,s}{\epsilon_{\text{avg}}(1-ms)} \tag{7}$$

Equation (7) differs from Equation (7*a*), which was incorrectly derived by Tiller and Cooper (*13*):

$$\frac{q_i}{q_1} = \frac{1-m_i s}{1-ms} \tag{7a}$$

The basic differential equation relating the flow rate q_x to the pressure gradient is

$$g_c \frac{dp_x}{dw_x} = -g_c \frac{dp_s}{dw_x} = \mu \alpha_x q_x \tag{8}$$

In terms of distance instead of the differential mass of solids per unit area dw_x, Equation (8) can be written in the form

$$g_c \frac{dp_x}{dx} = -g_c \frac{dp_s}{dx} = \mu \rho_s (1-\epsilon_x)\alpha_x q_x \tag{9}$$

Solving for p_x and integrating on the assumption of negligible p_1 yield

$$g_c \int_0^{p_x} dp_x = g_c p_x = \mu \rho_s \int_0^x (1-\epsilon_x)\alpha_x q_x\, dx \tag{10}$$

Integration through the entire cake and division of the result into Equation (10) lead to

$$\left(\frac{p_x}{p}\right)_T = \frac{\int_0^{x/L} (1-\epsilon_x)\alpha_x q_x d(x/L)}{\int_0^1 (1-\epsilon_x)\alpha_x q_x d(x/L)} \tag{11}$$

Equation (11) may be used in conjunction with Equation (6) to obtain the p_x distribution curve through the cake when a numerical process is adopted (*10*). A distribution for p_x/p vs. x/L is first assumed and thereby an ϵ_x vs. x/L curve is given. With Equation (6), q_x/q_1 is obtained as a function of x/L and substituted into Equation (11). The results are compared with the assumed p_x/p curve, and successive calculations are made until the desired accuracy is obtained. The true p_x distribution finally obtained is given a subscript T as presented in Equation (11).

In Figure 3 the three hydraulic-pressure distribution curves of the cement material predicted by Equations (2), (4), and (11) are shown in addition to the actual observed values. Although the experimental values obtained with the air-sealed manometers did not have a high degree of precision, Equations (2) and (11) gave the best correlation.

AVERAGE POROSITY

When the average porosity of a cake is constant, the mass w of dry solids per unit area may be related to the volume v of filtrate per unit area by the expression

$$w = \frac{\rho s}{1-ms} v \tag{12}$$

where m is the ratio of the mass of wet cake to the mass of dry cake. It is related to the average porosity ϵ_{avg} by

$$m = 1 + \frac{\rho\, \epsilon_{\text{avg}}}{\rho_s(1-\epsilon_{\text{avg}})} \tag{13}$$

As previously mentioned, the distribution for ϵ_x vs. x/L is obtained while obtaining the $(p_x/p)_T$ vs. (x/L) curve. Therefore, the average porosity may be obtained by integrating the ϵ_x curve throughout the entire cake:

$$(\epsilon_{\text{avg}})_T = \int_0^1 \epsilon_x\, d(x/L) \tag{14}$$

If it is assumed that the flow rate q_x is constant throughout the cake, the average porosity may be obtained from the expression

$$(\epsilon_{\text{avg}})_R = 1 - \frac{\int_{p_1}^{p} \frac{dp_x}{\alpha_x}}{\int_{p_1}^{p} \frac{dp_x}{\alpha_x(1-\epsilon_x)}} \tag{15}$$

Furthermore, if Kozeny's Law is assumed to be applied, Equation (15) becomes (16):

$$\epsilon'_{\text{avg}} = 1 - \frac{\int_{p_1}^{p} \frac{\epsilon_x^3}{(1-\epsilon_x)}\, dp_x}{\int_{p_1}^{p} \frac{\epsilon_x^3}{(1-\epsilon_x)^2}\, dp_x} \tag{16}$$

In addition to the use of Equations (14), (15), and (16), it is possible to employ the volume of filtrate vs. cake thickness data as shown in Figure 3 for calculating ϵ_{avg} or m. The mass of dry cake per unit area is given by

$$w = \rho_s(1-\epsilon_{\text{avg}})\,L \tag{17}$$

where L is a cake thickness at a time θ when the volume is v. Combining Equations (12), (13), and (17) yields

$$m_F = \frac{L/v + s\,(1-\rho/\rho_s)}{s\,(L/v+1)} \tag{18}$$

where m_F denotes the value of m obtained from L vs. v data. Values calculated on the basis of Equations (14), (15), (16), and (18) for the cement material filtered at $p = 7.11$ lb./sq. in. and $s = 0.384$ are respectively $m_T = 1.343$, $m_R = 1.342$, $m' = 1.335$, and $m_F = 1.361$. Furthermore, on the basis of p_x distribution data and with the setup shown in Figure 1, it is possible to obtain ϵ_x distribution with the compression data. The plot thus obtained is represented in Figure 3, and the calculation of average porosity of the cake is permitted. Integrating Figure 3 yields $m = 1.338$. All m values deviate from one another by less than a few percents.

The authors believe that the values which have just been calculated cannot be compared adequately with conventional, experimental measurements. Doubt exists concerning the accuracy of average porosity made on cakes taken from a filter press after the pressure has been released. It is well known that cake expansion occurs in different degrees. This effect has been reported in the literature (*10*) and was dramatically illustrated by Francis Hutto in time-lapse photography at the second filtration symposium of the American Institute of Chemical Engineers in Boston in 1956. In general, values of m determined by direct weighing are consistently higher than those obtained by calculation. It is the authors' opinion that calculated values of m are safer to use than those obtained from cakes removed from filter presses at the end of filtration.

EXPERIMENTAL DETERMINATION OF FILTRATION RESISTANCE

For the most part, experimental filtration resistances α_F have been obtained from constant pressure filtrations. Taking into account the variation in flow rate q with respect to distance throughout the cake, Tiller and Shirato (*15*) demonstrated that the conventional parabolic relation between volume and time should be modified. The basic differential equation may be placed in the form

$$\frac{dv}{d\theta} = \frac{g_c p}{\mu(J\alpha_R w + R_m)} \tag{19}$$

where α_R is the conventional Ruth filtration resistance defined by

$$\alpha_R = \frac{p - p_1}{\displaystyle\int_{p_1}^{p} \frac{dp_x}{\alpha_x}} \tag{20}$$

and J is a factor for correction due to nonuniform flow rate. The true filtration resistance $\alpha_T = J\alpha_R$; J is given by

$$J = \frac{1}{q_1 w}\int_0^w q_x\,dw_x = \frac{q_{\text{avg}}}{q_1} \tag{21}$$

where q_1 is the rate at the medium, and q_x is the variable rate throughout the cake. The filtration resistance α_R and α_T and the factor J will be constant throughout a constant pressure filtration only if p_1 is small. Replacing w in terms of v, assuming that the specific resistance remains constant, and integrating Equation (19) yield

$$v^2 + \frac{2(1-ms)R_m}{\alpha_F s\rho}\,v = \frac{2g_c p(1-ms)}{\mu\alpha_F s\rho}\,\theta = K\theta \tag{22}$$

The subscripted α_F indicates an experimentally determined value of α, which should equal $J\alpha_R$ of Equation (19). The Ruth coefficient K of time θ may be obtained from a plot of v vs. $\Delta\theta/\Delta v$. Then α_F is given by

$$\alpha_F = \frac{2g_c p(1-ms)}{\mu K s\rho} \tag{23}$$

While it has been abundantly demonstrated that K is constant, incorrect value of α_F will result if the wrong value of $(1-\text{ms})$ is employed. Correlation will also be poor for concentrated slurries if J is neglected (*15*). For dilute slurries, J and $(1-ms)$ are both approximately unity, and no problem presents itself.

On the contrary, in filtration of concentrated slurries the conventional methods of predicting both specific resistance α and moisture content of filter cake m should be corrected as demonstrated by Tiller and Shirato (*15*). It has been reported (*10*) that values of m determined by direct weighing are consistently higher, especially for the cakes filtered at high filtration pressure, than those obtained by calculation. Therefore, α_F should be determined with the reliable calculated values of m instead of the values determined by direct weighing.

CORRELATION BETWEEN THE CHARACTERISTICS OF THE MIXTURE AND ITS INGREDIENTS

Materials

To investigate the correlation between the filtration characteristics of slurry mixtures and their ingredients, a mixture of two slurries was employed. Each slurry contained a different compressible sludge respectively. Thus two different kaolin slurries (Mixture 1), a kaolin and gairome-clay slurry (Mixture 2), and clay and silica-sand slurry (Mixture 3) were used for this investigation. Mixture 1 contained slurries whose filtration characteristics are approximately the same, whereas Mixtures 2 and 3 contained slurries whose filtration characteristics are quite varied as shown in Table 1.

Porosity of Mixtures

Prediction of porosities of mixtures can be accomplished by assuming an additive law based on volume percentages.

TABLE 1. PROPERTIES OF MATERIAL USED

	Mixture 1		Mixture 2		Mixture 3	
	A	B	A	B	A	B
Density, ρ_s (g.-mass/cc.)						
	2.57	2.56	2.61	2.56	2.57	2.63
Stokes's diameter, analyzed by Andreasen's pippette						
$>20\mu$	11.2 wt. %	11.8 wt. %	0.5 wt. %	13.4 wt. %	4.9 wt. %	14.5 wt. %
$>10\mu$	27.4 wt. %	32.7 wt. %	5.0 wt. %	34.6 wt. %	12.0 wt. %	38.0 wt. %
$>5\mu$	42.2 wt. %	51.3 wt. %	15.0 wt. %	51.7 wt. %	25.8 wt. %	62.5 wt. %
$>2\mu$	56.5 wt. %	69.8 wt. %	31.0 wt. %	71.5 wt. %	45.5 wt. %	84.0 wt. %

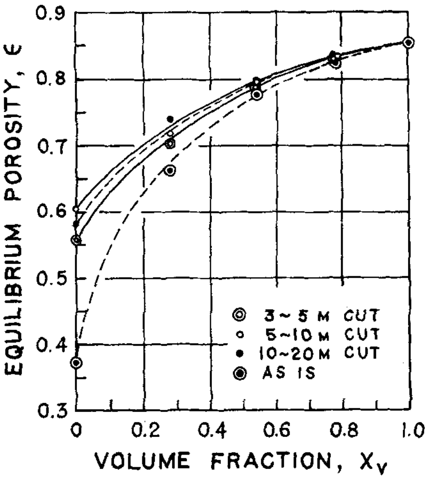

Fig. 4a. ε vs. X_v. Quartz and kieselguhr (Hoffing and Lockhart (4)).

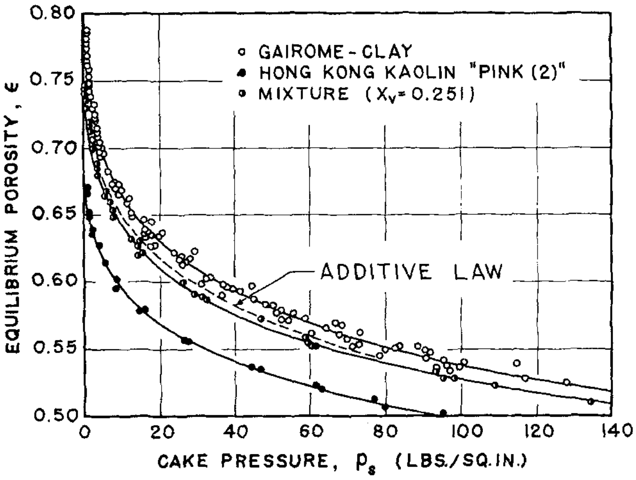

Fig. 5. ε vs. p_s. Mixture 2.

Consider 1 cu. ft. of solid material divided into two components as follows:

	First Component	Second Component
Mass fraction	X_w	$1-X_w$
Volume fraction	X_v	$1-X_v$
Porosity in pure state at a given pressure	ϵ_1	ϵ_2
Total volume in pure state due to component	$X_v/(1-\epsilon_1)$	$(1-X_v)/(1-\epsilon_2)$
Associated void volume	$\epsilon_1 X_v/(1-\epsilon_1)$	$\epsilon_2(1-X_v)/(1-\epsilon_2)$

The additive porosity ϵ_{xv} is given by the sum of the void volumes divided by the sum of the total volumes due to each component:

$$\epsilon_{xv} = \frac{\dfrac{\epsilon_1 X_v}{1-\epsilon_1} + \dfrac{\epsilon_2(1-X_v)}{1-\epsilon_2}}{\dfrac{X_v}{1-\epsilon_1} + \dfrac{1-X_v}{1-\epsilon_2}}$$

$$= \frac{X_v + \epsilon_2(1-\epsilon_1)/(\epsilon_1-\epsilon_2)}{X_v + (1-\epsilon_1)/(\epsilon_1-\epsilon_2)} \quad (24)$$

It is apparent that an additive law does not lead to a linear relation in X_v.

In Figure 4a data obtained by Hoffing and Lockhart (4) are shown. The porosity of various mixtures of quartz and diatomaceous earth is plotted against the volume fraction of diatomaceous earth. The four lines represent calculations made in accord with the additive law developed in Equation (24). The porosity is not linear in the volume fraction even though the additive law holds. Although Hoffing and Lockhart reported that the addition of a small amount of diatomaceous earth to the quartz resulted in a remarkable increase in porosity, the increase is simply a result of the additive law. In Figure 4b the porosity of Mixture 2 is plotted against the volume fraction of the denser material, Honk Kong pink kaolin. The dotted lines represent predictions based on the additive law. Experimental values were smaller by 4% as a maximum deviation than those predicted on the basis of the additive law as shown in Figure 4b and 5. This is probably owing to

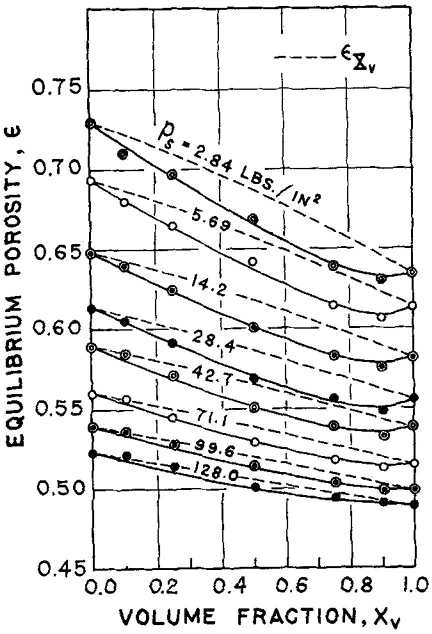

Fig. 4b. ε vs. X_v. Mixture 2.

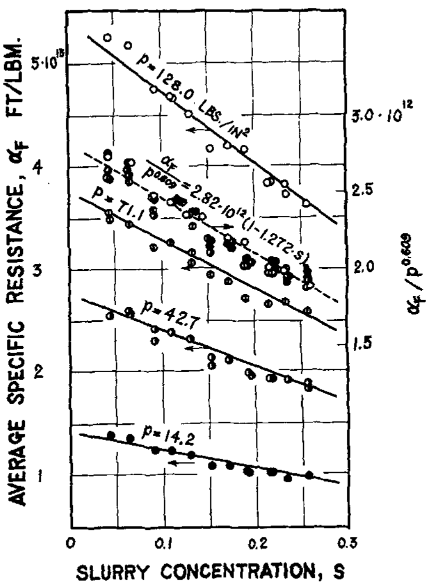

Fig. 6. α_F vs. s. Gairome clay Mitsukuri (Mixture 2, X_w = 0).

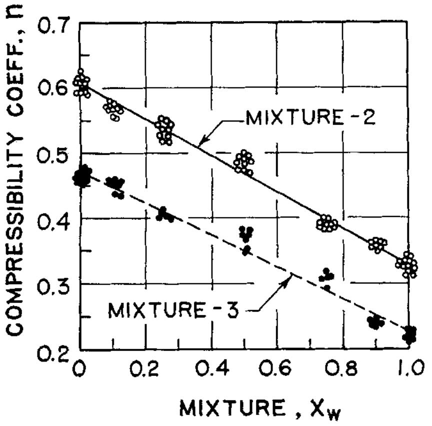

Fig. 7. n vs. X_w. Mixtures 2 and 3.

the fact that small particles of one of the ingredients fill the voids of the other. Hoffing and Lockhart (*4*) reported similar results. Where the additive law did not represent the behavior, the experimental porosities were lower than the predicted values.

Average Specific Resistance

Average specific resistance α_F was obtained from various constant pressure filtration of the slurry of each ingredient and mixture. In Figure 6, the average specific resistance of Gairome-clay Mitsukuri (Mixture 2, $X_w = 0$) is plotted against slurry concentration s. An increase in the slurry concentration s gradually causes a decrease in the average specific resistance. In Figure 6, α_F/p^n is also plotted against s, where n is the so-called *compressibility* coefficient of the filter cake.

Thus, an empirical expression may be written as

$$\alpha_F = \alpha_o\,(1 - \phi \cdot s)\,p^n \tag{25}$$

The empirical expression (25) deviated less than 5% from almost all the results of more than 500 filtration runs. Theory indicates that ϕ would change when s approaches the point where the slurry becomes semisolid. The compressibility coefficient n plotted against the mass fraction X_w was approximately linear as shown in Figure 7.

The plots of average specific resistance of a mixture of two clays α_F against the mass fraction X_w are shown as a family of curves as in Figure 8. If one follows the concepts by Grace (*3*) and Tiller (*11*) and defines S as the average effective specific surface area, the following equation will result:

$$(k \cdot S^2)^{1/2} = \left\{ \frac{\alpha_F \cdot \rho_s \displaystyle\int_0^p \frac{\epsilon_x^3}{1-\epsilon_x}\,dp_x}{p} \right\}^{1/2} \tag{26}$$

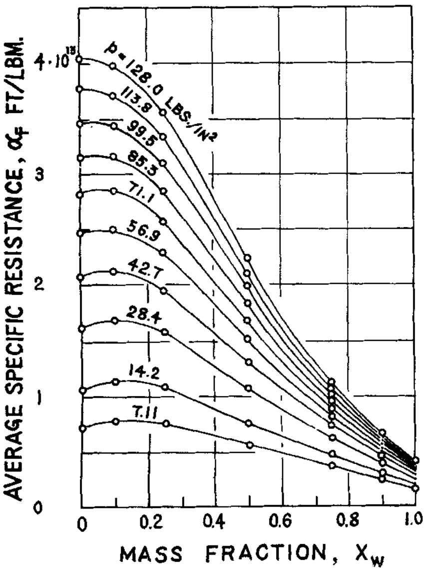

Fig. 8. α_F vs. X_w. Mixture 2, s = 0.200.

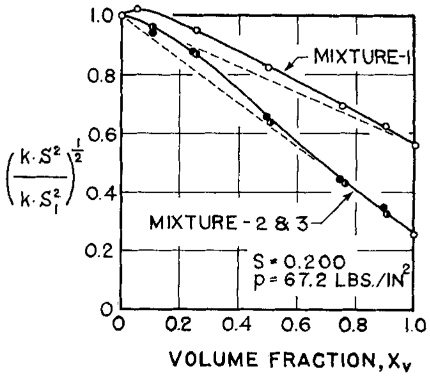

Fig. 9. $(kS^2/kS_1^2)^{1/2}$ vs. X_v. Mixtures 1, 2, and 3.

The plots of $(k \cdot S^2)^{1/2}$ of a mixture divided by $(k \cdot S_1^2)^{1/2}$ of one component of the mixture against the volume fraction X_v were close to a linear relation or the additive law by a maximum difference of 10% throughout Mixtures 1, 2, and 3, as shown in Figure 9. This deviation seems to be small, but it must be remembered that in filtration equations the specific surface area always appears in the form of S^2 instead of S.

Figure 10 shows filtration results and the values predicted both by the conventional Ruth theory and by the additive law. As far as Mixtures 1, 2, and 3 of clay slurries are concerned, the filtration characteristics determined when the existence of the additive law was assumed were fairly comparable to the filtration results with a maximum difference of about 20%.

CONCLUSIONS

1. It has been indicated that experimentally determined values of ϵ_{avg} or m for a cake will be incorrect if there is cake expansion on removal of the pressure. It is suggested that adequate values of ϵ_{avg} or m may be obtained from volume vs. cake thickness data, porosity distribution as determined from hydraulic pressure measurements, or data obtained from a compression-permeability cell.

2. It was shown that filtration resistance varies markedly with slurry concentration. Values predicted on the basis

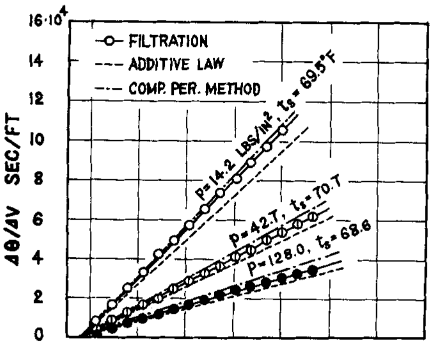

Fig. 10. $\Delta\theta/\Delta v$ vs. v. Mixture 3, $X_w = 0.10$, $s = 0.200$.

of the conventional Ruth's equation are only valid for dilute slurries.

3. It seems logical to assume that the average effective specific surface areas of a mixture of slurries should be additive, but $(k \cdot S^2)^{1/2}$ vs. X_v is slightly concave upwards for compressible clay systems.

4. It may be supposed that, when the particle size distributions of the precipitates of two slurries are approximately the same, the equilibrium porosity of the mixed sludge is fairly equal to the simple additive value, and, when the particle size distributions are considerably different, the equilibrium porosity of the mixed sludge is less than the additive value. This is probably owing to the fact that the solids of the smaller ingredient will fill the voids created by the solids of the larger ingredient. The compressibility coefficient vs. the mass fraction X_w is fairly linear throughout Mixtures 1, 2, and 3.

5. As far as the mixtures of clay-slurries are concerned, it is safe to say that variation of filtration resistances and porosities follow approximately the additive law.

ACKNOWLEDGMENT

The prime author wishes to thank the National Science Foundation for a grant which made preparation of this paper possible and to express his appreciation for help in preparing this manuscript given by Dr. Frank M. Tiller, Dean of Engineering, University of Houston. The author was awarded a Fulbright travel grant under the sponsorship of the United States Department of State Educational Exchange Program. The author wishes to thank the University of Houston, The Filter Product Division of Johnson and Johnson, The Duriron Company, and The Industrial Filter and Pump Manufacturing Company for their support.

NOTATION

A = cross-sectional area, sq. ft.
g_c = conversion factor, poundals/lb.-force
J = correction factor defined by Equation (21), dimensionless
k = Kozeny's Constant, dimensionless
K = Ruth's coefficient per unit area in constant pressure equation, $v^2 = k\theta$, sq. ft./sec.
L = cake thickness, ft.
m = ratio of wet to dry cake mass, dimensionless
m' = value of m calculated on the basis of Equation (16), dimensionless
m_F = value of m obtained from filtration experiment defined by Equation (18), dimensionless
m_R = value of m predicted by compression permeability experiment on the basis of Equation (15), dimensionless
m_T = true value of m predicted by compression permeability experiment, dimensionless
n = compressibility coefficient, dimensionless
p = applied filtration pressure, lb.-force/sq. ft.
p_s = cake compressive pressure at distance x from the medium lb.-force/sq. ft.
p_x = hydraulic pressure at distance x from the medium, lb.-force/sq. ft.
p_1 = pressure at the interface of medium and cake, lb.-force/sq. ft.
q_x = rate of flow of liquid in cake at distance x from the medium, cu. ft./(sq. ft.) (sec.)
q_1 = value of q_x at the medium, cu. ft./(sq. ft.) (sec.)
q_{avg} = average value of q_x defined by Equation (21), cu. ft./(sq. ft.) (sec.)
R_m = medium resistance, 1/ft.
s = solids fraction in slurry, dimensionless
S = average effective specific surface area of cake solids defined by Equation (26), sq. ft./cu. ft.
S_o = effective specific surface area of cake solids, sq. ft./cu. ft.
t_s = temperature of filtrate, °F.
v = volume of filtrate per unit area, cu. ft./sq. ft.
V = volume of filtrate, cu. ft.
w = total mass of dry solids per unit area, lb.-mass/sq. ft.
w_x = mass of solids per unit area in distance x from the medium, lb.-mass/sq. ft.
x = distance from the medium, ft.
X_v = volume fraction of one component to the total solids in the mixture, dimensionless
X_w = mass fraction of one component to the total solids in the mixture, dimensionless

Greek Letters

α = specific filtration resistance, ft./lb.-mass
α_F = value of α determined by filtration experiment, defined by Equation (23), ft./lb.-mass
α_R = value of α defined by Equation (20), ft./lb.-mass
α_T = true value of α defined by $\alpha_T = J \cdot \alpha_R$, ft./lb.-mass
α_x = local value of α at cake pressure p_s, ft./lb.-mass
α_o = constant defined by Equation (25)
ϵ = equilibrium porosity at cake pressure p_s, dimensionless
ϵ_x = local value of porosity at distance x from the medium, dimensionless
ϵ_{avg} = average porosity of entire cake, dimensionless
ϵ_{avgx} = average porosity for cake lying between medium and distance x, dimensionless
ϵ'_{avg} = average porosity of entire cake calculated by Equation (16), dimensionless
ϵ_{xv} = porosity of mixture predicted by Equation (24), dimensionless
ϵ_1 = equilibrium porosity of first component at a given pressure, dimensionless
ϵ_2 = equilibrium porosity of second component at a given pressure, dimensionless
θ = time, sec.
μ = viscosity, lb.-mass/(ft.) (sec.)
ρ = density of liquid, lb.-mass/cu. ft.
ρ_s = true density of solids, lb.-mass/cu. ft.
ϕ = constant defined by Equation (25)

LITERATURE CITED

1. Carman, P. C., *Trans. Inst. Chem. Engrs.*, (*London*), **15**, 150 (1937); **16**, 168 (1938).
2. Collins, R. E., "Flow of Fluids Through Porous Materials," Reinhold, New York (1961).
3. Grace, H. P., *Chem. Eng. Progr.*, **49**, 303, 367 (1953).
4. Hoffing, E. H., and F. J. Lockhart, *Chem. Eng. Progr.*, **47**, 3 (1951).
5. Hoffing, E. H., *ibid.*, p. 10 (1951).
6. Ingmanson, W. L., *Chem. Eng. Progr.*, **49**, 11 (1953).
7. Kozeny, J., *Sitzber. Akad. Wiss.*, *Wien*, *Abt.* IIa,, **136**, 271 (1927).
8. Leo, M. A., *Chem. Eng. Progr.*, **47**, 10 (1951).
9. Ruth, B. F., *Ind. Eng. Chem.*, **38**, 564 (1946)
10. Shirato, Mompei, and Sakio Okamura, *Chem. Eng.* (*Tokyo*), **19**, 111 (1955); **20**, 98 (1956).
11. Tiller, F. M., *Chem. Eng. Progr.*, **49**, 467 (1953); **51**, 282 (1955).
12. ———, *A.I.Ch.E. Journal* **4**, 170 (1958).
13. ———, and H. R. Cooper, *ibid.*, **6**, 595 (1960).
14. —————, *ibid.*, **8** (September, 1962).
15. Tiller, F. M., and Mompei Shirato, submitted to *A.I.Ch.E. Journal*.

Manuscript received July 25, 1962; revision received February 6, 1963; paper accepted February 8, 1963. Paper presented at A.I.Ch.E. New Orleans meeting.